Computational Fluid Dynamics Modeling of Downward Bubbly Flows

Mahmood Reza Rahimi, Hajir Karimi

Abstract—Downward turbulent bubbly flows in pipes were modeled using computational fluid dynamics tools. The Hydrodynamics, phase distribution and turbulent structure of two-phase air-water flow in a 57.15 mm diameter and 3.06 m length vertical pipe was modeled by using the 3-D Eulerian-Eulerian multiphase flow approach. Void fraction, liquid velocity and turbulent fluctuations profiles were calculated and compared against experimental data. CFD results are in good agreement with experimental data.

Keywords—CFD, Bubbly flow, Vertical pipe, Population balance modeling, Gas void fraction, Liquid velocity, Normal turbulent stresses.

I. INTRODUCTION

TURBULENT bubbly flows in pipes exist in many industries applications such as power, chemical, food, pharmaceutical industrials. Knowledge of the interaction between the bubbles and the turbulent flow is of great significance for the design and operation of these applications. Gas–liquid two-phase flow exists in a wide variety of forms, depending on the flow rates of phases, the physical properties of the phases, the geometry and orientation of the pipe. The different interfacial structures are called flow patterns or flow regimes. Vertical two-phase flows are usually classified into four basic flow regimes consist of bubbly flow, slug flow, churn turbulent flow and annular flow [1]. In the bubbly flow, liquid phase is continuous and small dispersed bubbles flow within the liquid. This flow regime is widely take place in many devices in chemical, petroleum, mining, food and pharmaceutical industries. The uncertainty in bubble flow occur from a lack of essential understanding of the local hydrodynamics and rate processes, which govern bubble size and thus the interfacial area between phases.

In dispersed gas-liquid flows, the bubble size distribution plays an important role in the phase structure and interphase forces, which, in turn determine the multiphase hydrodynamic behaviours, including the spatial profiles of the gas fraction, gas and liquid velocities, and mixing and mass-transfer behaviours. These influences must be taken into account for obtaining good predictions in wide operating conditions when using computational fluid dynamics (CFD) simulation. The population balance model (PBM) is an effective technique to simulate the bubble size distribution. The PBM was first

M. R. Rahimi and H. Karimi are with the Chemical engineering department, Yasouj University, Yasouj 75918-74831 Iran.
(e-mail: mrrahimi@mail.yu.ac.ir).

formulated for chemical engineering purposes by Hulburt and Katz [2]. The population balance model has been used extensively for modeling of different processes. The discrete bubble sizes prescribed in the dispersed phase were tracked by solving an additional set of transport equations, which these equations were progressively coupled with the flow equations during the simulations. Few attempts have been reported on the modeling of turbulent two phase bubbly flows [3-9].

Currently, upward flows were studied most extensively in a broad range of publications [1, 3–9]. Downward flows were investigated more scantily, especially by CFD models combined with population balance modeling. The main aim of this work is to examine the ability of proposed CFD model coupled with population balance modeling, especially for showing phase distribution, turbulent structure and liquid phase velocity. In this study turbulent bubbly air/water two-phase flows in a circular pipe were investigated. The internal phase distribution of air-water bubbly flow in a 57.15 mm diameter 3.06 m length vertical downward pipe has been modeled using the 3-D Eulerian-Eulerian multiphase flow approach combined with Population Balance Modeling (PBM). Important flow quantities such as local void fraction, liquid velocity and the turbulent fluctuations were calculated and compared against experimental data of Wang et al. [10].

II. MODELING

The numerical simulations presented here are based on the two-fluid, Eulerian–Eulerian model where is based on ensemble-averaged mass and momentum transport equations for each phase. Regarding the liquid phase (α_l) as the continuous and the gas phase (bubbles) as the dispersed phase (α_g), these equations, without interface heat and mass transfer, can be written as follows:

Continuity equation of the liquid phase:

$$\frac{\partial}{\partial t}(\rho_l \alpha_l) + \nabla.(\rho_l \alpha_l \mathbf{u}_l) = 0 \tag{1}$$

Continuity equation of the gas phase

$$\frac{\partial}{\partial t}(\rho_g \alpha_g f_i) + \nabla.(\rho_g \alpha_g \mathbf{u}_g f_i) = S_i \tag{2}$$

where f_i is the volume fraction of bubbles of group i and S_i is a source term that takes into account the death and birth of bubbles caused by coalescence and break-up processes. $S_i = 0$ under the assumption of constant and uniform bubble size

and zero interphase mass transfer. In this study S_i is calculated as

$$S_i = B_i^B + B_i^C - D_i^B - D_i^C \qquad (3)$$

where i varies from 1 to N (i =1,2,...,N) and B^B, B^C, D^B and D^C are respectively, the 'birth' and 'death' due to break-up and coalescence of bubbles. The production rates due to coalescence and break-up and the death rate due to coalescence and break-up of bubbles formulated as

$$P_i^C = \frac{1}{2}\sum_{k=1}^{N}\sum_{l=1}^{n}\chi_{i,kl}n_i n_j \qquad (4a)$$

$$D_i^C = \sum_{j=1}^{n}\chi_{ij}n_i n_j \qquad (4b)$$

$$P_i^C = \sum_{j=1}^{n}\Omega(V_j:V_i)n_j \qquad (4c)$$

$$D_i^B = \Omega_i n_i \qquad (4d)$$

The bubble number density n_i is related to the gas volume fraction α_g by $\alpha_g f_i = n_i V_i$ where V_i is the corresponding volume of a bubble of group i. The break-up of bubbles in turbulent dispersions employs the model developed by Luo and sevendsen [13] and the coalescence rate considering turbulent collision by Prince and Blanch [14].

The momentum conservation for multiphase flows is described by the volume averaged momentum equation as follows:

$$\frac{\partial}{\partial t}(\rho_k \alpha_k u_k) + \nabla.(\rho_k \alpha_k u_k u_k) = -\alpha_k \nabla p + \qquad (5)$$

$$\rho_k \alpha_k g - \nabla(\tau_k \alpha_k) + F_{km} \quad (k,m=l,g)$$

where $\mathbf{u}$ is the volume averaged velocity vector, p is the pressure, g is the gravity, τ_k is the phase shear stress tensor $(\tau_k = -\mu_k(\nabla \mathbf{u}_k + \nabla \mathbf{u}_k)^T)$ and $\mathbf{F}_{km}$ is the interphase force term. The terms on the right-hand side describes the following forces acting on the phase k: the pressure gradient, gravity, the viscous stress term and interphase momentum forces combined in $\mathbf{F}_{km}$. The pressure is defined to be equal in both phases. The effective viscosity μ_k of the viscous stress term consists of the laminar viscosity and an additional turbulent part in case of turbulence. The total interfacial force acting between two phases is the sum of several independent physical effects:

$$F_{km} = F_D + F_L + F_{VM} + F_{WL} + F_{TD} \qquad (6)$$

The forces indicated above respectively represent the interphase drag force $\mathbf{F}_D$, lift force $\mathbf{F}_L$, virtual mass force $\mathbf{F}_{VM}$, wall lubrication force $\mathbf{F}_{WL}$, and turbulence dispersion force $\mathbf{F}_{TD}$. Detailed descriptions of each of these forces can be found in Anglart and Nylund [17]; Lahey and Drew [18] and Joshi [19]. In this model the drag force, lift force, wall lubrication force and turbulence dispersion forces are considered into account. The drag force density is written in the following form:

$$F_D = \frac{3}{4}C_D \alpha_d \rho_c \frac{1}{d_b}|u_c - u_d|(u_c - u_d) \qquad (7)$$

Where C_D is the drag coefficient taking into account the character of the flow around the bubble and d_b is the bubble diameter. The drag coefficient C_D in Eq. (7) has been modeled using drag model of Ishii-Zuber [20]. The lift force considers the interaction of the bubble with the shear field of the liquid. It acts perpendicular to the main flow direction and is proportional to the gradient of the liquid velocity field. The lift force in terms of the slip velocity and the curl of the liquid phase velocity can be modeled as [21–24]:

$$F_L^c = -F_L^d = C_L \alpha_d \rho_c (u_c - u_d) \times \nabla \times u_c \qquad (8)$$

Where C_L is the lift coefficient and the subscripts c and d stands for the continuous and dispersed phases. The turbulent dispersion force, derived by Lopez de Bertodano [25], as

$$\mathbf{F}_{TD}^c = -\mathbf{F}_{TD}^d = -C_T \rho_c k_c \nabla \alpha_c \qquad (9)$$

Where k_c is the liquid turbulent kinetic energy per unit of mass. Liquid flow rate between bubble and the wall is lower than between the bubble and the outer flow, and this is the origin of the wall lubrication force. This results in a hydrodynamics pressure difference driving bubble away from the wall. This force density is expressed by Antal et al. [26] as:

$$F_{WL}^c = -F_{WL}^d = -\alpha_g \rho_l \frac{u_r - (u_r n_w)n_w)^2}{d_b} \qquad (10)$$

$$\max[C_1 + C_2 \frac{d_b}{y_W}, 0]n_W$$

here, $\mathbf{u}_r = u_c - \mathbf{u}_d$ is the relative velocity between phases, d_b is the disperse phase mean diameter, y_w is the distance to the nearest wall, and n_w is the unit normal pointing away from the wall. The local Sauter mean diameter of bubbles based on the calculated values of the scalar fraction f_i and discrete bubble sizes d_i can be deduced from:

$$d_b = \frac{1}{\sum f_i / d_i} \qquad (11)$$

Turbulence is taken into consideration for the continuous phase using k-ε model and the influence of the dispersed phase on the turbulence of the continuous phase is taken into account with the Sato's bubble-induced turbulent viscosity model [11]. The governing equations for the turbulent kinetic energy k and turbulent dissipation ε are:

$$\frac{\partial}{\partial t}(\rho_l \alpha_l k) + \frac{\partial}{\partial x_i}.(\rho_l \alpha_l u_l k) = \frac{\partial}{\partial x_i}(\alpha_l(\mu_l + \frac{\mu_{l,tur}}{\sigma_k})\frac{\partial k}{\partial x_i}$$

$$+ \alpha_l(G - \alpha_l \rho_l \varepsilon_l)$$

$$\frac{\partial}{\partial t}(\rho_l \alpha_l \varepsilon_l) + \frac{\partial}{\partial x_i}.(\rho_l \alpha_l u_l \varepsilon_l) = \frac{\partial}{\partial x_i}(\alpha_l(\mu_l + \frac{\mu_{l,tur}}{\sigma_\varepsilon})\frac{\partial \varepsilon_l}{\partial x_i})$$

$$+ \alpha_l \frac{\varepsilon_l}{k}(C_{\varepsilon 1}G - C_{\varepsilon 2}\alpha_l \rho_l \varepsilon_l)$$

$$\mu_{l,tur} = C_\mu \rho_c \frac{k_c^2}{\varepsilon_c} \qquad (12)$$

Where $C_{\varepsilon 1}$, $C_{\varepsilon 2}$, C_μ, σ_k, σ_ε are the standard $k - \varepsilon$ model constants and G is the turbulence production term. Using the standard $k - \varepsilon$ model the turbulent viscosity of the continuous phase is calculated by

$$\mu_{\alpha,eff} = \mu_{\alpha,lam} + \frac{\mu_{\alpha,tur}}{\sigma_k} \qquad (13)$$

III. EXPERIMRNT

An air/water loop was used by Wang et al. [10] had a 57.15 mm diameter and 3.06 m length test section for measurements of both up and down flows. A single sensor cylindrical hot-film probe was used to measure the mean and fluctuations in the axial liquid velocity and the local void fraction. Reynolds stress components in the liquid phase, measured using a special 3-D conical probe. One eighth of a pipe using symmetry boundary conditions for both axial cut planes was used in order to reduce the computational costs. A typical grid structure is shown in Fig. 1. The first layer in inflated layer near the wall was set at a distance from the wall to take a value of the y^+ in the range from 30 to 40, in order to achieve stable solutions avoiding numerical oscillations and also to have an accurate wall lubrication force modeling.

IV. SOLUTION METHOD

CFD analysis was carried out using commercial CFD software. The simulations were carried out as 3-D downward flow in a vertical pipe based on the Eulerian–Eulerian description combined with Population Balance Modeling (PBM). Conservation equations are discretised using finite volume method, upwind scheme was used for all equations, SIMPLEC algorithm was used for pressure-velocity coupling. Water was considered as the continuous phase, and air as the dispersed phase. In this study, bubbles are equally divided into 5 classes. The PBM model has been used to account for the non-uniform bubble size distribution in a gas–liquid mixture.
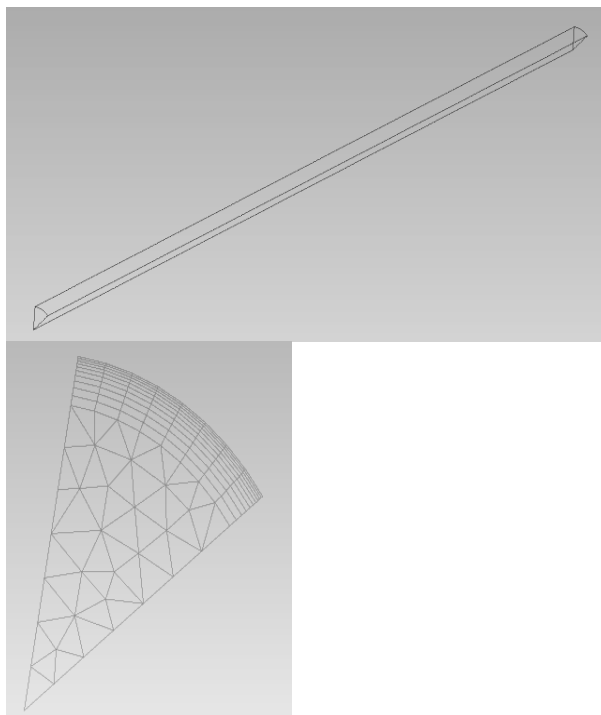

Fig. 1 Grid structure.

The following boundary conditions were used in this study. For the pipe inlet boundary condition, uniform gas and liquid velocities and average volume fractions have been specified; a relative average static pressure of zero was specified at the pipe outlet boundary condition. Symmetry boundary conditions were used for both axial cut planes. No slip boundary conditions were used at wall. Average volume fraction and uniform liquid velocity profile are specified for initiating the numerical solution. Several grids were used in order to set up the computational domain. The best computational time and also independency of the results from the calculation grid was examined for different grids. Several simulations were done using gradually larger number of grid points starting from about 30000, there was seen practically no change in the gas volume fraction and liquid velocity profiles when the grid size increased beyond 120000. The mathematical model was applied in the CFD commercial code for numerical studies, with the construction of a particular numerical grid and with its own subroutine in Fortran language for the closure equations of model.

V. RESULTS AND DISCUSION

The proposed model was tested by using this model for an air/water flow system used by Wang et al. [10] had a 57.15 mm internal diameter. The predicted values of gas void fraction were presented in Figure 2. The results are follows the correct trend, as can be seen in this figure. It was found that the void fraction profile showed a distinct peak near the wall that means bubbles tended to migrate toward the wall. It was also shown that the observed wall peaking and coring

phenomena, and thus the radial void distribution, can be predicted. Fig. 2 shows the void fraction distributions obtained from the model comparing with the measured data at the dimensionless axial position z/D = 35. From the phenomenological view point, the phase distribution patterns along the radial direction of the bubble column exhibits four basic types of distributions: "wall peak", "intermediate peak", "core peak" and "transition", as categorised by Serizawa and Kataoka[12]. In the bubbly flow regime, maximum void fraction located close to the wall demonstrated the flow phase distributions typically known as the "wall peak" behavior, which was mainly due to the positive lift force pushing the small bubbles toward the pipe wall. As depicted in Fig. 2, a well-developed wall peaking behavior was recorded in the experiment and had been successfully captured by the model. For higher liquid flows it was found that "wall-peaking" became more pronounced. The predictions are in good agreement with measurements within the error bands, but the discrepancy occurred close to the wall. Overally the peaking and coring of void fraction are well-predicted using this combined CFD- PBM model of this study. Fig. 3 shows the local radial liquid velocity distributions at z/D = 35 for two cases involving liquid single phase flow and two phase flow with specified gas and liquid superficial velocities. The simulation results of liquid velocity profiles obtained from this modeling as depicted in Fig. 3 compared with measurements and were found to be in good agreement with the experimental data. Although the liquid velocities at the core were still over predicted for the case of two-phase flow with Jg=0.1m/s. Normal turbulent fluctuations predicted by this modeling is shown in Fig. 4 in comparison with measured data. All Reynolds stress components were measured using a special 3-D conical probe Wang et al.[10]. In two-phase flows, the normal Reynolds stress components (i.e. u'^2, v'^2 and w'^2) showed nearly flat profiles in the core region (r/R < 0.8) and, except near the wall, the turbulence structure was more anisotropic compared to single-phase flows[10]. Normally, the presence of the bubbles increased the level of turbulence in the flow.

However, because the bubbles in turbulent two-phase flow enhance dissipation as well as promoting the production of turbulence kinetic energy, it was found that for higher flow rates the presence of bubbles suppressed the level of turbulence. In two-phase flows, the presence of voids tends to flatten the liquid velocity profile for both up and down flows. Moreover, for high flows in the upward direction the location of the maximum liquid velocity occurred off the pipe's centerline. But the maximum liquid velocity and the void peak did not occur at the same location, probably because of the counteracting effect of high shear stress near the wall as shown
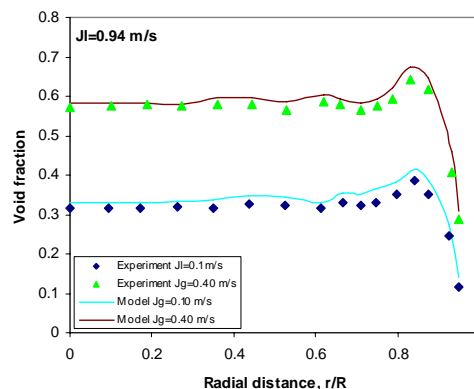

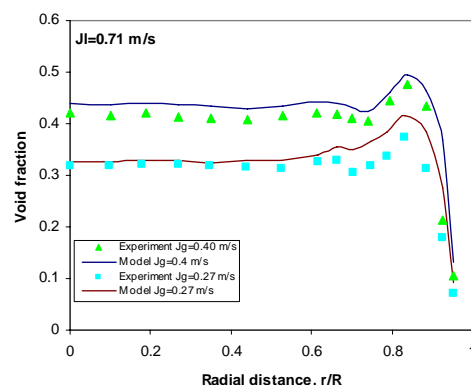Fig. 2 Gas void fraction in comparison with experimental data of Wang et.al.[10].

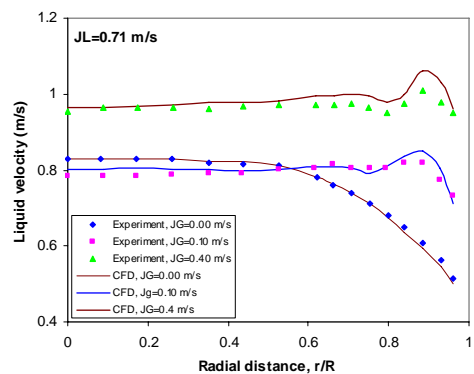Fig. 3 Gas void fraction in comparison with experimental data of Wang et.al.[10].

Fiq. 4 Local radial liquid velocity distributions at z/D = 35.

by Wang et. al.[10]. The void fraction profile exhibited a sharp peak near the wall. The liquid velocity profile was flattened by the presence of the vapor phase (i.e. the bubbles). However, a "chimney effect", in which the maximum liquid velocity occurs away from the pipe's center, was observed. Moreover, all three normal fluctuations were affected by the presence of the vapor phase. These fluctuations do not increase monotonically as the void fraction increases.
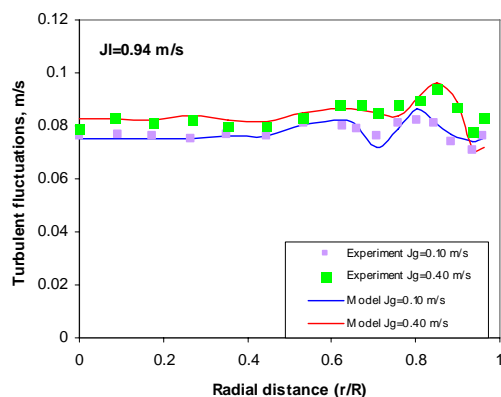
Fig. 5 Predicted turbulent fluctuations in comparison with measured data of Wang et. al.[10], z/d=35.

VI. CONCLUSION

Turbulent bubbly air/water two-phase flows in a circular pipe were investigated. The internal phase distribution air-water bubbly flow in a 57.15 mm i.d. 3.06 m length vertical pipe has been modeled using the 3-D Eulerian-Eulerian multiphase flow approach combined with Population Balance Modeling (PBM). Important flow quantities such as local void fraction, liquid velocity and the Reynolds stresses were calculated and compared against experimental data of Wang et. al.[10]. The void fraction profile exhibited a sharp peak near the wall. The liquid velocity profile was flattened by the presence of the vapor phase (i.e. the bubbles). However, a "chimney effect", in which the maximum liquid velocity occurs away from the pipe's center, was observed. Moreover, all three normal fluctuations were affected by the presence of the vapor phase. These fluctuations do not increase monotonically as the void fraction increases. In the core region, the normal turbulent fluctuations and the void fraction frequently showed flat profiles.

REFERENCES

[1] H. Karimi, M. R. Rahimi, "A Robust Classification method for the Prediction of Two Phase Flow Pattern, using Ensemble Classifiers Technique," *in proc. 11th Int. Conf. on Multiphase Flow in Industrial Plants*, Palermo, 2008, pp. 443-451.

[2] H. Hulburt, S.Katz, "Some Problems in Particle Technology: a Statistical Mechanical Formulation," *Chem. Eng. Sci,* vol. 19, 555, 1964.

[3] G. Kocamustafaogullari, M. Ishii, "Foundation of the interfacial area transport equation and its closure relations," *Int. J. Heat Mass Trans*, vol. 38 (3), pp. 481–493, 1995.

[4] T. Wang, J. Wang, and Y. Jin, "Population Balance Model for Gas−Liquid Flows: Influence of Bubble Coalescence and Breakup Models," *Ind. Eng. Chem. Res.,* vol. 44, 19, 2005.

[5] T. Hibiki, M. Ishii, Z. Xiao, "Axial interfacial area transport of vertical bubble flows," *Int. J. Heat Mass Trans,* vol. 44, pp 1869–1888, 2001.

[6] T. Hibiki, M. Ishii, "Development of one-group interfacial area transport equation in bubbly flow systems," *Int. J. Heat Mass Trans*., vol. 45, pp. 2351–2372, 2002.

[7] K. Ekambara, R.S. Sanders, K. Nandakumar, J.H. Masliyah, "CFD simulation of bubbly two-phase flow in horizontal pipes," *Chem. Eng. J.,* vol. 144, pp. 277–288, 2008.

[8] C.P. Cheung, G.H. Yeoh,, J.Y. Tu, "On the modeling of population balance in isothermal vertical bubbly flows – Average bubble number density approach," *Chem. Eng. Process.*, vol. 46, pp. 742–756, 2007.

[9] S. Sarı, S. Ergün, M. Barık, C. Kocar, C. N. Sökmen, "Modeling of isothermal bubbly flow with ınterfacial area transport equation and bubble number density approach," *Annals of Nuclear Energy* , vol. 36, pp. 222-232, 2009.

[10] S. K. Wang, S. J. Lee, O. C. Jones and R. T. Lahey, "3-D turbulece structure and phase distribution measurements in bubbly two-phase flows," *Int. J. Multiphase flow*, Vol. 13, pp. 327-343, 1987.

[11] Y. Sato, M. Sadatomi, K. Sekoguchi, "Momentum and heat transfer in two-phase bubbly flow—I," *International Journal of Multiphase Flow*, vol. 7, pp. 167–178, 1981.

[12] A. Serizawa, I. Kataoka, "Phase distribution in two-phase flow. In: Afgan, N.H. (Ed.), *Transient Phenomena in Multiphase Flow*. Washington, DC, pp. 179–224, 1988.

[13] H. Luo, H. Svendsen, "Theoretical model for drop and bubble break-up in turbulent dispersions, *AIChE J.*, vol. 42, pp. 1225–1233, 1996.

[14] M.J. Prince, H.W. Blanch, "Bubble coalescence and break-up in air sparged bubble columns," *AIChE J.,* vol. 36, pp. 1485–1499, 1990.

[15] A.K. Chesters, G. Hoffman, "Bubble coalescence in pure liquids," *Appl. Sci. Res*, vol. 38, pp. 353–361, 1982.

[16] J.C. Rotta, *Turbulente Stromungen*, Stuttgart, 1974.

[17] H. Anglart, O. Nylund, "CFD application to prediction of void distribution in two-phase bubbly flows in rod bundles," *Nucl. Sci. Eng.*, vol. 163, pp. 81–98, 1996.

[18] R.T. Lahey Jr., D.A. Drew, "The analysis of two-phase flow and heat transfer using multidimensional, four field, two-fluid model," *Nucl. Eng. Des.*, vol. 204,pp. 29–44, 2001.

[19] J.B. Joshi, "Computational flow modeling and design of bubble column reactors," *Chem. Eng. Sci*., vol. 55, pp. 5893–5933, 2001.

[20] M. Ishii, N. Zuber, "Drag coefficient and relative velocity in bubbly, droplet or particulate flows," *AIChE J.*, vol. 25, pp. 843–855, 1979.

[21] I. Zun, "The transverse migration of bubbles influenced by walls in vertical bubbly flow," *Int. J. Multiphase Flow*, vol. 6, pp. 583–588, 1980.

[22] N.H. Thomas, T.R. Auton, K. Sene, J.C.R. Hunt, "Entrapment and transport of bubbles by transient large eddies in turbulent shear flow, *in proc. BHRA International Conference on the Physical Modelling of Multiphase Flow,* 1983.

[23] D.A. Drew, S.L. Passman, *Theory of Multicomponent Fluids*, Springer-Verlag, New York, 1999.

[24] A. Tomiyama, H. Tamai, I. Zun, S. Hosokawa, "Transverse migration of single bubbles in simple shear flows," *Chem. Eng. Sci.*, vol. 57, pp. 1849–1858, 2002.

[25] M.A. Lopez de Bertodano, "Turbulent bubbly two-phase flowin a triangular duct, Ph.D. dissertation, Rensselaer Polytechnic Institute, 1992.

[26] S.P. Antal, R.T. Lahey, J.E. Flaherty, "Analysis of phase distribution in fully developed laminar bubbly two phase flow," *Int. J. Multiphase Flow,* vol. 7, 635, 1991.